Processing Seismic Ambient Noise Data with the Continuous Wavelet Transform to Obtain Reliable Empirical Green's Functions

Yang Yang[1]

Chunyu Liu[1]

Charles A. Langston[1]

[1]Center for Earthquake Research and Information
University of Memphis
3876 Central Ave., Suite 1
Memphis, TN 38152

Submitted to the
Geophysical Journal International
on August 17, 2019
Under second review on Feb. 20, 2020

Running title: Processing Seismic Ambient Noise Data with the CWT

Yang.Yang@memphis.edu
cliu5@memphis.edu
clangstn@memphis.edu

SUMMARY

We propose a new data processing flow to compute empirical Green's functions (EGF) from ambient seismic noise based on a soft thresholding designaling and denoising method using the continuous wavelet transform. The designaling algorithm is carried out during the initial data processing to remove earthquakes and other transient signals in the seismic record. A continuous wavelet transform denoising algorithm removes the noise in the final stacked cross-correlogram. The overall data processing procedure is divided into four stages: (1) single station data preparation, (2) remove earthquakes and other signals in the seismic record, (3) spectrum whitening, cross-correlation and temporal stacking, (4) remove the noise in the stacked cross-correlogram to deliver the final EGF. The whole process is automated to make it accessible for large datasets. Synthetic data constructed with a recorded earthquake and recorded ambient noise is used to test the designaling method. We then apply the new processing flow to data recorded by the USArray Transportable Array stations near the New Madrid Seismic Zone where many seismic events and transient signals are observed in the data. We compare the EGFs calculated from our new flow with time domain normalization and our results show improved signal-to-noise ratios and deliver more reliable measurements that can be used for further processing. The designaling method improves the homogeneity of the ambient noise wavefield which is an intrinsic requirement for seismic interferometry. The final denoising step suppresses random noise and provides clearer EGFs for the next processing step.

Keywords: Seismic interferometry, seismic noise, wavelet transform

INTRODUCTION

Cross-correlation of diffuse wave fields, such as from ambient noise or scattered coda waves, can be used to estimate the medium Green's function termed the empirical Green's function (EGF) between a pair of stations (e.g. Shapiro et al. 2005; Sabra et al. 2005; Wapenaar & Fokkema 2006). This method has been widely applied to data collected in different regions over the past 15 years to extract surface waves and body waves. Densely deployed networks have provided an opportunity for high-resolution surface wave tomography (e.g. Yao et al. 2006; Lin et al. 2008; Bensen et al. 2008) and full waveform inversion (e.g. Gao & Shen 2014; Emry et al. 2018). In spite of these applications, there have been fewer efforts to develop improved ambient noise data processing procedures in order to acquire more reliable and higher signal-to-noise ratio (SNR) EGFs. Bensen et al. (2007) summarized and compared different procedures on the use of seismic records to obtain surface wave dispersion measurements and their suggestions are still the main procedures that are generally used today to process ambient noise data.

Ground motion produced by earthquakes and other sources, such as non-stationary noise sources near a station or weather storm signals, will be recorded on the seismogram and are often considered as "useful signals" that contain important information about the seismic source and underground structure. However, in ambient noise tomography, these signals destroy the diffuse wave field assumption and need to be considered as "noise" in correlation processing. One of the most important steps during the processing is to remove these signals to obtain as "pure" ambient noise as possible. In Bensen et al. (2007), this step is called "time-domain normalization" or "temporal normalization", which is a procedure for reducing the effect of earthquakes, instrumental irregularities and non-stationary noise sources near to stations on the cross-correlations. This process balances the amplitude of ambient noise relative to the amplitude of unwanted signals. Here, “signal” and “noise” are related to what is being studied and depend on whether removing “signal” or “noise” is useful for our purpose. Earthquakes and other source “signals” should be removed before cross-correlation because large amplitude signals at zero-delay time in the cross-correlation disguise the surface wave arrival from the microseisms. To avoid confusion, based on the common way of naming “ambient noise”, we call the removing of earthquakes and other non-stationary noise source “signals” as designaling in this paper although the mathematics of doing so is the same as denoising.

Bensen et al. (2007) summarized different methods for identifying and removing earthquakes and other contaminants from the original recordings. These include 1-bit normalization, running absolute mean normalization and water level normalization that all suppress the contaminating signals. However, amplitude information is not fully retained in the cross-correlation because of the inherent amplitude down-weighting process in these methods. Amplitude is of fundamental importance for body wave anelastic attenuation estimation and basement resonance estimation based on the horizontal to vertical amplitude ratio (H/V ratio) of surface waves. Bensen et al. (2007) also suggested using running absolute mean normalization as the best practice to process the ambient noise data. In the rest of this paper, we will call this method as “time domain normalization” and it will be used as the benchmark method for comparison.

Removing transient signals while not touching the ambient noise itself is a crucial requirement for successful ambient noise data processing. We propose a method based on the Continuous Wavelet Transform (CWT) for dealing with this problem. The CWT has been widely used to for seismic analysis and denoising purposes (Pazos et al. 2003; Chik et al. 2009; To et al. 2009; Ansari et al. 2010; Beenamol et al. 2012; Mousavi & Langston 2016; Mousavi et al. 2016).

Compared with other denoising methods, using the CWT to achieve denoising has many natural translation-invariant and time-frequency properties such as reducing pseudo-Gibbs artifacts in the denoised signal (Elad & Aharon, 2006). In ambient noise data, the noise record usually dominates the time series with earthquakes or other transient signals contaminating only a small portion of the whole record. The statistical properties of the ambient noise can be estimated based on a segment of the noise record and time-frequency CWT analysis allows us to navigate the rest of data and remove the unwanted signals. The CWT provides one of the best choices for ambient noise designaling. Unlike its normal purpose for removing noise, we use this method in a reverse manner to take the signal out and keep the background ambient noise.

The motivation of this paper is to introduce a designaling procedure based on the CWT and apply it to ambient noise data processing. We also use essentially the same method to remove noise in the final stacked cross-correlograms. Details of the designaling and denoising methods will be given and then explored using a synthetic data example. Next, we use our new ambient noise processing flow to process data collected from EarthScope's USArray Transportable Array within the northern Mississippi embayment. The New Madrid Seismic Zone (NMSZ) inside of the Mississippi embayment is one of the most earthquake-active intraplate regions in North America (Hildenbrand, 1985; Cox et al., 2001; Tuttle et al., 2002; Thomas, 2006; Van Arsdale et al., 2007; Powell et al., 2010; Dunn et al., 2013; Van Arsdale and Cupples, 2013; Nyamwandha et al., 2016; Yang & Langston, 2019). Abundance of seismic events in the NMSZ could be used to test the efficiency and robustness of our method. Using the real data, the resulting EGFs and the final dispersion curves obtained from our method and Bensen's method are compared.

CWT DENOISING AND DESIGNALING

CWT

The CWT (Daubechies 1992) is a popular tool to study time-frequency representations of continuous or discrete time series. This mathematical transformation decomposes a signal into different scales as a function of time. Different scales provide different resolutions (or can be considered as different pseudo-frequency components) of the original signal. From this point of view, it provides better resolution compared to the short time Fourier transform (Tary et al. 2014). Assuming we have a time series $s(t)$, for a given mother wavelet $\psi(t)$, the CWT of time series $s(t)$ at scale a $(a > 0)$ and time shift b can be expressed as (Daubechies 1992)

$$Ws(a,b) = \int_{-\infty}^{+\infty} s(t) a^{-1/2}\, \psi^{*}\left(\frac{t-b}{a}\right) dt, \tag{1}$$

where the $*$ indicates the complex conjugate and $Ws(a,b)$ is the wavelet coefficient representation of the signal $s(t)$ at scale a and time shift b. The Fourier transform of the mother wavelet $\psi(t)$ should satisfy the admissibility condition (Daubechies 1992; Farge 1992)

$$0 < C_{\psi} = \int_{-\infty}^{+\infty} |\omega|^{-1} \left|\hat{\psi}(\omega)\right|^{2} d\omega < \infty, \tag{2}$$

in which $\hat{\psi}(\omega)$ is the Fourier transform of the mother wavelet $\psi(t)$ and C_{ψ} is called the wavelet admissibility constant. Such a wavelet is called an admissible wavelet. An admissible wavelet also implies that $\hat{\psi}(0) = 0$ so that the integration over time must be zero (Daubechies 1992). To recover the original signal from the CWT representations, the inverse CWT can be expressed as

$$s(t) = \frac{1}{C_{\psi}} \int_{0}^{\infty} \int_{-\infty}^{+\infty} \frac{1}{\sqrt{a}} Ws(a,b)\, \psi\left(\frac{t-b}{a}\right) \frac{da db}{a^{2}}. \tag{3}$$

The CWT of a discrete time series can be expressed in the similar way by replacing integration with summation (Torrence & Compo 1998) and different fast algorithms are developed to make it computation affordable (Rioul & Duhamel 1992). In another mathematical view of equation (1), the CWT can be considered as a cross-correlation of the target time series $s(t)$ with different wavelets that are stretched or compressed and shifted versions of the selected mother wavelet $\psi(t)$. Because of this cross-correlation property, the CWT can be calculated using the fast Fourier transform (FFT) in the frequency domain (Daubechies 1992). The CWT spectrum $Ws(a,b)$ for the time series $s(t)$ is the time-frequency decomposition of the original signal, with different scales a analogous to wave period (inverse frequency) and b indicating time lag.

Designaling and denoising via soft thresholding

Langston & Mousavi (2019) discussed an efficient method based on the CWT to denoise or designal a time series using the statistical estimation of the noise. In this study, we implement the soft thresholding method in the ambient noise data processing flow. Essentially, the noise is estimated and then removed for different scales of wavelets by a less severe manner. The size of datasets used for ambient noise tomography is usually very large. Thus, processing ambient noise data requires an algorithm that is not time-consuming and works efficiently. Soft thresholding (Weaver et al., 1991) can remove noise efficiently compared to computationally intensive block thresholding algorithms on the wavelet scale-time plane (Mousavi & Langston, 2016).

In order to apply the CWT soft thresholding denoising, the original time series $s(t)$ is first transformed into the CWT time-frequency domain to get the CWT spectrum $Ws(a,b)$. The noise level for a specific scale a is estimated and the CWT coefficients for this scale are modified by the non-linear soft thresholding given by

$$\bar{W}s(a,b) = \begin{cases} sign[Ws(a,b)](\|Ws(a,b)\| - \beta(a)) \; if \; \|Ws(a,b)\| \geq \beta(a) \\ 0 \qquad otherwise \end{cases}, \tag{4}$$

where

$$sign[Ws(a,b)] = \frac{Ws(a,b)}{\|Ws(a,b)\|}, \tag{5}$$

$\bar{W}s(a,b)$ is the CWT spectrum after denoising for the scale a and $\|\cdot\|$ stands for the modulus of the complex spectrum in the CWT domain. The threshold function $\beta(a)$ is determined based on the statistics of the absolute value of the noise for scale a. If the CWT spectrum is less than $\beta(a)$, it is considered as the noise and we will remove it by setting it to zero. Otherwise, it contains both noise and signal, and the predefined noise is subtracted from the original spectrum. This criterion is applied to data at each scale in the CWT spectrum. Ambient noise data is continuously recorded and earthquakes and other signals only make up a small proportion of the whole record. The noise level $\beta(a)$ can be well estimated with a predetermined time segment which contains only ambient noise. Much of the signal processing procedures start from an assumption of Gaussian noise. The threshold function can be computed using the mean and standard deviation of the CWT spectrum for scale a within the selected time segment:

$$\beta(a) = mean(\|Ws(a,b)\|) + N \; std(\|Ws(a,b)\|), \tag{6}$$

where

$$mean(\|Ws(a,b)\|) = \frac{1}{T_2 - T_1}\int_{T1}^{T2} \|Ws(a,b)\| \, db, \tag{7}$$

$$std(\|Ws(a,b)\|) = [\frac{1}{T_2 - T_1}\int_{T1}^{T2} (\|Ws(a,b)\| - mean(\|Ws(a,b)\|))^2 \, db]^{\frac{1}{2}}, \tag{8}$$

and N is a parameter that controls the threshold noise level. The time limits T_1 and T_2 represent the start and end time of the selected time segment.

There are different criteria to choose the threshold coefficient, N, in equation (6). Simply choosing $N = 3$ will yield a signal at 99.7% confidence level (Starck et al., 2010) if the CWT coefficients of the noise follow a normal distribution. This method is straightforward to estimate the noise level. But unfortunately, the assumption that the CWT coefficients follow a Gaussian distribution is rarely seen in seismic noise data (Langston & Mousavi, 2019). The distribution for real ambient noise is usually unpredictable. However, we can estimate a data-driven noise level by taking the approach of empirically estimating the cumulative distribution of noise and then calculating the 99% confidence value for the distribution. To calculate the empirical cumulative distribution function (ECDF), we can order the N samples noise values and then assign a probability jump of 1/N when a value is attained, starting with the smallest value. Thus, the threshold function becomes:

$$\beta(a) = \mathrm{ECDF}^{-1}(P = 0.99), \tag{9}$$

where ECDF$_{-1}$ is the inverse of the cumulative distribution function or the quantile.

In Fig. 1, we compare the threshold functions assuming Gaussian statistics in equation (6) Fig.1 and non-Gaussian statistics in equation (9). The distribution of the empirical probability distribution function of the real noise is different compared to a Gaussian distribution and gives quite different estimated noise levels. Overall, there are significant differences between the ECDF and Gaussian threshold functions. It also suggests that the ECDF method would lead to a better estimate of the threshold and thus we use the ECDF method to estimate the noise level in our processing.

Designaling reverses the denoising process. This procedure can be applied in our ambient noise processing to remove earthquakes and other signals. For the soft thresholding case, signal is removed by using

$$\bar{W}s(a,b) = \begin{cases} sign[Ws(a,b)]\beta(a) \; if \; \|Ws(a,b)\| \geq \beta(a) \\ \quad Ws(a,b) \qquad\qquad otherwise \end{cases}. \tag{10}$$

At each scale, if the CWT spectrum is less than the estimated noise level, we consider it as the noise and keep the spectrum. Otherwise, we consider it as the signal and remove it by setting the coefficient to the noise level.

Using the soft thresholding method to remove noise or signal based on ECDF is very straightforward and efficient. After applying equation (4) for denoising or equation (10) for designaling, we get our new CWT spectrum and get the final denoised or designaled output for our next processing step by doing the inverse CWT from equation (3).

DATA AND DATA PROCESSING FLOW

Data preprocessing

We use data from 55 broadband seismic stations of EarthScope's USArray Transportable Array (TA) recorded during July, 2012, within and around the northern Mississippi embayment (Fig. 2) to demonstrate our ambient noise data processing flow. Velocity models for this area are developed using full waveform tomography of the EGFs extracted from all temporary and permanent stations. The crustal and upper mantle structures underneath the northern Mississippi embayment are investigated. These models will be the subject of future reports.

Fig.2

In order to compare the robustness of our method, we compare cross-correlations and dispersion curves with those computed based on time domain normalization (TDN). The "MSNoise" package (Lecocq et al., 2014) is a python package which implements the TDN method.

We first download daily vertical component waveform data for each station through the IRIS (www.iris.edu) FDSN web service and work with them in SAC format, remove the instrument response, remove the mean and trend, apply a bandpass filter from 0.02Hz to 1Hz and downsample the sampling rate from 40Hz to a 5Hz. The reason why we choose the passband 0.02-1Hz is that previous studies (e.g. Liang et al., 2008; Langston et al., 2009; Liu et al., 2018a; Yang & Langston, 2019) observed prominent surface wave arrivals in this frequency band. Downsamping the sampling rate to 5 Hz not only reduces the storage but also reduces the computation time of cross-correlations. Small events are usually higher frequency and are filtered out during the downsampling.

CWT ambient noise data processing flow

The temporal normalization step is replaced by the designaling method described above. After single station data preparation, the CWT designaling method is applied on each day of the data, followed by spectral whitening to provide spectrum-balanced data. A 5% taper is applied at the beginning and end of each data segment to avoid artifacts during cross-correlation. Each pair of stations are then cross-correlated and all one-day cross-correlograms for the month are stacked to increase the SNR.

In order to estimate the noise statistics for each day, we need to find a segment of the data that only contains noise. This is realized by a simple algorithm. For each day's data, we divide the time series into 48 half hour segments. The maximum absolute value in each segment is determined and the segment with the minimum absolute value is chosen to estimate noise statistics. There is no guarantee that earthquakes or other signals will not appear within the selected segment, but it provides a fast and accurate way to find this estimate. The time duration for each segment could be shorter when teleseismic events occur more frequently but each segment still needs to be long enough to make a robust estimate. The test in Fig. 2 shows that the noise level could be estimated accurately with data time series as short as 500 seconds.

Besides removing the signal, soft thresholding can also be used to remove the noise in the final stacked EGFs to increase the SNR (equation 4). This step is applied to deliver the final EGFs.

Our new ambient noise data processing flow can be summarized into the following steps:

Step 1: Pre-processing: prepare waveform data for each station individually, which includes cutting the data into intervals of one-day, removing the instrument response, removing the mean and trend, applying a bandpass filter and resampling the data to a 5Hz sampling rate.

Step 2: Designal: for each one-day time series for a station, apply the soft thresholding designaling method to remove earthquakes and other transients.

Step 3: Spectral whitening, cross-correlation and stack: applying spectral whitening for each one-day time series for a station to provide a broader-band and spectrum-balanced data. Calculate the cross-correlation for each possible day and each station pair. Stack the desired number of day-correlations for each station.

Step 4: Applying the soft thresholding denoising method to remove the noise in each of the stacked cross-correlograms.

After step 4, we get the final EGFs for a pair of station, which can then be used to measure group and phase velocity (Liu et al., 2019) or to do full waveform tomography (Yang & Langston, 2019) to determine earth structure.

RESULTS

We first apply the designaling algorithm to "synthetic" seismic data constructed from real data. The whole designaling procedure can be better examined and compared with the known noise input signal. Next, the entire flow will be applied to our subset of the TA array data and compared with results from using TDN.

In our implementation of the CWT, we use the Morlet wavelet as the mother wavelet $\psi(t)$ in equation (1) and (3) with 16 voices per octave. The designaling method is not sensitive to the number of the decomposition levels and smaller scale numbers will speed up the whole processing (Mousavi and Langston, 2016). Using 16 voices per octave in the processing is large enough for resolution while retaining efficiency. Choosing the right mother wavelet is also a difficult task. Different target problems require different optimal wavelets. We tried a number of different mother wavelets and by comparing the RMS error between the input noise and the final designaled results from the synthetic test, we achieve the least misfit using the Morlet wavelet. Therefore, we will use the Morlet wavelet in our data processing.

Synthetic Data

To best simulate real data, we construct a synthetic time series by using two segments of recorded seismograms at station U41A. One segment contains 3,000 seconds of ambient noise data. The other seismogram segment is with the same length but contains a teleseismic event. The ambient noise segment is chosen to make sure that there is no earthquake or other obvious transient signal in the selected time period by looking at the seismogram in the time domain and the scalogram in the CWT domain. A teleseismic event occurred on July 25, 2012, was recorded by the station and is used as the earthquake input. The soft thresholding denoising algorithm is first applied on the earthquake segment to remove any ambient noise contained in the seismogram. Then, both the ambient noise segment and the denoised earthquake segment are filtered with a 1Hz low-pass filter. The earthquake segment is then tapered before the first arrival time and at 1400 seconds to make sure there is no noise or signal before or after. The ambient noise segment and the teleseismic event segment are then summed to produce the final synthetic data (Fig. 3). Fig.3

The CWT spectrum of the synthetic data is calculated and shown in Fig. 3(d). The earthquake and ambient noise are clearly distinguished and are indicated in the spectrum. The CWT spectrum for ambient noise only falls into a specific range of scales and keeps a very stable amplitude pattern. These scales correspond to the main frequency band of the ambient noise. The earthquake contains signals over a wider range of scales which corresponding higher scale or lower frequency data and with much larger amplitude. The CWT spectrum for the earthquake is also changing with time and the pattern looks irregular. The overlapping scale band between the earthquake data and the ambient noise data makes it impossible to separate them by just using a bandpass filter.

After 1500 seconds, the seismogram is pure ambient noise and we use this segment to calculate the ECDF of the ambient noise and estimate the noise level for each scale. After obtaining the statistical properties of the ambient noise, we will decide whether the CWT spectrum is kept the same or modified by using the criteria in equation (10). The CWT spectrum after soft thresholding and the final designaled seismogram are shown in Figs 3e and f. The designaling algorithm removes most of the earthquake signal and the noise superficially looks the same before and after designaling. The time series after designaling looks more like the original ambient noise since it has a balanced amplitude throughout. A comparison of particular time windows before and after designaling is also shown in Figs 3g and h. Noise is not modified by this algorithm and appears qualitatively the same before and after designaling. The CWT spectrum of the designaled time series is like a clipped version of the original spectrum which suggests that there is still some small effects of the teleseism in the time series. We compare the Fourier amplitude spectrum of input noise, input synthetic data and final designaled results (Fig. 4). The designaled time series has a slightly larger amplitude spectrum than the original spectrum of the input noise due to the existence of some signals. But overall, the designaled result shows very good amplitude recovery.

Fig. 4

Real Data

All of data recorded by the selected TA stations during July 2012 are used as input data to test the new processing flow. We will use the station V44A (Fig. 2) which is located within the NMSZ as an example to show the results. There are plenty of earthquakes and transient signals appearing in the original recording (Fig. 5), which make it perfect to test the new processing flow. For comparison, we also process the same data with TDN as a benchmark.

Fig. 5

Station V44A and S38A are used to show the details of each processing step (Fig. 6). A teleseismic event is obviously present in these particular data. Ambient noise is barely seen and is buried beneath the earthquake signals. Earthquake signals are efficiently removed after soft threshold designaling and we get an amplitude-stable time series. Both stations show similar results and no obvious earthquakes or transient signals are seen in the data after designaling.

Fig. 6

The designaled data are then correlated. The cross-correlogram from the soft thresholding designaled data has higher SNR compared with the one from TDN. The Rayleigh wave at positive time lags is not clearly seen in the result using TDN. The running absolute mean normalization method will only balance the amplitude of the original data to match the amplitude of the ambient noise. However, the spectrum is dominated by the truncation of peaks and troughs of the high amplitude signal in the time domain that non-linearly increases its high frequency parts. Truncating the CWT is less severe because individual wavelets are intrinsically smooth and are smoothed yet again during the inverse transform integration. The data of the two stations for other days are processed in the same way and the final one-month stacked cross-correlogram calculated from our processing flow also shows higher SNR (Fig. 6d). The designaling method removes earthquakes and other transient signals in a physical meaningful way and it does not touch any ambient noise data. TDN achieves temporal normalization but modifies the ambient noise while using a relatively harsh way to balance the amplitude of the whole time series. We suggest that CWT designaling preserves more of the noise characteristics within the event time window.

After correlation and stacking, random noise is still clearly seen in the stacked EGF. To further increase the SNR, we apply soft threshold denoising on the stacked EGF (Fig. 6e). This will remove much of the noise within the final stacked cross-correlogram and give us an even higher SNR result.

A more dramatic example is shown in Fig. 7. One-month correlation results are stacked Fig. 7
for stations W42A and W46A to get the EGF. Fourier filtering and the soft threshold denoising method are applied to improve the SNR of the stacked EGF. The noise frequency range overlaps with the signal frequency range. After the low-pass filter, noise is still obvious in the EGF and the SNR does not increase significantly. However, with the soft threshold denoising method, the noise is removed and the denoised EGF has a very high SNR, which provides for better input in later processing steps, such as group and phase velocity extraction.

Fig. 8 shows a record section of final EGFs for master station V44A from our processing Fig. 8 flow and TDN. Both processing flows give clear EGFs. Symmetric Rayleigh waves are also observed. To better compare the two processing flows quantitatively, we compute the SNR by using the ratio of maximum amplitude between -200s and 200s and the maximum amplitude for the rest of data. Our new processing flow gives five to ten times higher SNR over using TDN. Rayleigh waves are clearly observed on both positive and negative time lags with smaller amplitude noise in between.

The next step after acquiring the final EGFs is to calculate phase or group velocities between each station pair. Althought this is not the primary purpose of this paper, it is useful to examine the differences in results obtained using the two data processing schemes. Readers may refer to other studies and reports (e.g. Yao et al., 2006; Bensen et al., 2007) for more details of dispersion calculation. Here, we show a comparison of the group velocities determined from EGFs between the two processing flows for one station pair (Fig. 9). We calculated the group Fig. 9 velocity dispersion curve for station S38A using frequency-time analysis (Dziewonski et al., 1969). Although group velocities have significant overlap between the two methods, they clearly have different trends for periods greater than 15s. It is likely that these changes in the dispersion curves will give rise to differnces in the resulting velocity models.

DISCUSSION

When deciding which processing flow to use for a specific dataset, we should observe how many earthquakes and other transient signals are contained in the data. In the interest of computational efficiency, if there are few transient events then CWT designaling may be overkill, wasting valuable compute cycles.

The new processing flow will deliver reliable and high SNR EGFs, which will be very helpful in further processing steps, such as studying the attenuation or extracting body waves from ambient noise seismic interferometry. However, some drawbacks of our processing flow still need to be considered. The main concern is its relatively high computational cost. The CWT is the most time-consuming part, which requires many forward and inverse Fourier transforms. When processing large datasets such as years of ambient noise recording from large networks, the computational time to designal will not be insignificant. Based on our processing experience, it will take about half a minute to designal one-day of data for one station on a Macbook Pro laptop. One possible solution is to use graphic processor unit (GPU) to calculate the wavelet transform and remove the signals when processing large amounts of data, which will speed up the processing significantly. It will take about 8 seconds to designal one-day of data for all 55 stations on a NVDIA V100 GPU. Another possibility is to check the data first and only apply the soft threshold designaling if signals are observed in the data. In this study, we only processed one-month of data at 55 stations and the time for the processing is acceptable.

Another assumption for this method is that the ambient noise time series should be stable in that its statistical properties should not change significantly in each one-day data segment. If such changes are observed in the data, the largest noise level should be used in the designaling process to avoid accidentally removing any ambient noise.

Ambient noise tomography has been widely used during the last 15 years and will be continuously developed in the future. Acquiring more reliable EGFs and getting more information from seismic interferometry will make this method more powerful and robust.

CONCLUSIONS

We propose a new ambient noise data processing flow to compute reliable EGFs. The denoising and designaling algorithm is based on the CWT with soft thresholding and is essential to this flow. The whole processing flow is automated without any manual interference. The new processing flow is suitable for data containing regional and teleseismic events or other transient signals. The whole processing flow is divided into four steps: (1) single station data preparation, (2) remove earthquakes and other transient signals in the seismic record, (3) spectrum whitening, cross-correlation and temporal stacking, (4) remove the noise in stacked cross-correlogram to deliver the final EGFs. The final EGFs can be used to extract phase or group velocity or to invert for velocity structure by full waveform tomography.

The principal step during data preparation is to acquire pure ambient noise that is free of earthquake and other transient signals (instrument irregularities and non-stationary noise sources near to stations, etc.). We adopt a method based on the CWT to remove these unwanted signals. The intrinsic time-frequency property of the CWT makes it possible to isolate noise and signal efficiently. A segment of pure ambient noise is usually obtainable and can be used to estimate the statistical property of the noise in the CWT domain. The estimated noise statistical properties are then used as a guide to detect whether the data point at different time and scales in the CWT domain is noise or not. A soft thresholding method is used to remove the signal if the data exceeds the noise level. We constructed synthetic data based on recorded noise and an earthquake to successfully test the method. Use on more extensive data shows excellent signal removal. Other denoising algorithms based on the CWT such as block thresholding (Mousavi et al., 2016) could also be used to remove earthquakes and other signals in the time series but they also require much more computational cost. Our method is efficient for large datasets.

The denoising method can also be used to remove the noise in the final EGFs to further increase the SNR. We use the same algorithm as in the designaling step but in a reverse manner to significantly increase the SNR in the final EGF. This denoising method performs better than bandpass filters since a Fourier filter has no time resolution.

We applied our processing flow to one-month of data from EarthScope TA stations near the NMSZ. Many earthquakes and other transient signals were recorded by the stations which make this dataset an appropriate test dataset for the algorithm. We obtain better EGFs with higher SNR than results using TDN. Except for removing earthquake and other transient signals that obscure the ambient noise data, and noise removal for the final stacked empirical Green's function, our processing flow is basically the same as previously proposed (Bensen et al., 2007). In regions where few earthquakes occur, there should not be many differences in the resulting EGFs between these two processing flows. However, the stacked EGF denoising step is recommended for both methods because it has relatively low computational cost but dramatically increases the SNR.

DATA AND RESOURCES

Seismogram data used in this study are collected from IRIS (http://www.iris.edu, last accessed on January 2019). A MATLAB GUI code to process simple dataset and visualize the results from the CWT denoising and designaling method used in this study can be accessed at http://www.ceri.memphis.edu/people/clangstn/software.html (last accessed on August 2019). A CPU/GPU code to process large ambient noise datasets can be downloaded from https://github.com/SwiftHickory/bc_denoise.git (last accessed on August 2019).

ACKNOWLEDGEMENT

We are grateful for financial support from the Center for Earthquake Research and Information to perform this research. This research was supported by the Air Force Research Laboratory under contract FA9453-18-C-0064.

REFERENCE

Ansari, A., Noorzad, A., Zafarani, H. & Vahidifard, H., 2010. Correction of highly noisy strong motion records using a modified wavelet denoising method, Soil Dynam. Earthq. Eng., 30, 1168–1181.

Beenamol, M., Prabavathy, S. & Mohanalin J., 2012. Wavelet based seismic signal de-noising using Shannon and Tsallis entropy, Comput. Math. Appl., 64, 3580–3593.

Bensen, G. D., Ritzwoller, M. H., & Shapiro, N. M., 2008. Broadband ambient noise surface wave tomography across the United States, J. Geophys. Res., 113(B5).

Bensen, G. D., Ritzwoller, M. H., Barmin, M. P., Levshin, A. L., Lin, F., Moschetti, M. P., ... & Yang, Y., 2007. Processing seismic ambient noise data to obtain reliable broadband surface wave dispersion measurements, Geophys. J. Int., 169(3), 1239-1260.

Chik, Z., Islam, T., Rosyidi, S. A., Sanusi, H., Taha, M. R. & Mustafa, M. M., 2009. Comparing the performance of Fourier decomposition and wavelet decomposition for seismic signal analysis, Eur. J. Scientif. Res., 32, 314–328.

Cox, R. T.,Van Arsdale, R. B. & Harris, J. B., 2001. Identification of possible Quaternary deformation in the northeastern Mississippi Embayment using quantitative geomorphic analysis of drainage-basin asymmetry, Geol. Soc. Am. Bull., 113(5), 615-624.

Daubechies, I., 1992. Ten Lectures on Wavelets, Vol. 61, SIAM, Philadelphia, Pennsylvania, 357 pp., doi: 10.1137/1.9781611970104.

Dunn, M., DeShon, H. R., & Powell, C. A., 2013. Imaging the New Madrid seismic zone using double-difference tomography, J. Geophys. Res., 118(10), 5404-5416.

Dziewonski, A.M., Bloch, S. & Landisman, M., 1969. A technique for the analysis of transient seismic signals, Bull. Seism. Soc. Am., 59, 427– 444.

Elad, M., & Aharon, M., 2006. Image denoising via sparse and redundant representations over learned dictionaries, IEEE Trans. Image Process., 15, 3736–3745.

Emry, E. L., Shen, Y., Nyblade, A. A., Flinders, A. & Bao, X., 2018. Upper Mantle Earth Structure in Africa From Full-Wave Ambient Noise Tomography, Geochemistry, Geophysics, Geosystems, 20(1), 120-147.

Farge, M., 1992. Wavelet transforms and their applications to turbulence, Annu. Rev. Fluid Mech., 24, 395–458, doi: 10.1146/annurev.fl.24.010192.002143.

Gao, H., & Shen, Y., 2014. Upper mantle structure of the Cascades from full-wave ambient noise tomography: Evidence for 3D mantle upwelling in the back-arc, Earth and Planetary Science Letters, 390, 222-233.

Hildenbrand, T. G., 1985. Rift structure of the northern Mississippi embayment from the analysis of gravity and magnetic data, J. Geophys. Res., 90(B14), 12607-12622.

Johnston, A. C., & Schweig E. S., 1996. The enigma of the New Madrid earthquakes of 1811-1812, Anna. Rev. Earth Planet. Scie., 24, 339-384.

Langston, C. A., & Mousavi, S. M., 2019. Separating signal from noise and from other signal using non-linear thresholding and scale-time windowing of continuous wavelet transform, Bull. Seism. Soc. Am., accepted for publication.

Langston, C. A., Chiu, S. C. C., Lawrence, Z., Bodin, P., & Horton, S., 2009. Array observations of microseismic noise and the nature of H/V in the Mississippi embayment, Bulletin of the Seismological Society of America, 99(5), 2893-2911.

Lecocq, T., Caudron, C. & Brenguier, F., 2014. MSNoise, a python package for monitoring seismic velocity changes using ambient seismic noise, Seismological Research Letters, 85(3), 715-726.

Liang, C., & LangstonC. A, 2008. Ambient seismic noise tomography and structure of eastern North America. J. Geophys. Res., 113(B3).

Lin, F. C., Moschetti, M. P. & Ritzwoller, M. H., 2008. Surface wave tomography of the western United States from ambient seismic noise: Rayleigh and Love wave phase velocity maps, Geophys. J. Int., 173(1), 281-298.

Liu, C., Langston, C. A. & Powell C. A., 2019. Crustal and uppermost mantle shear wave velocity and radial anisotropy beneath the Missisippi embayment from ambient noise tomography, manuscript submitted for publication.

Mousavi, S. M. & Langston, C. A., 2016, Hybrid Seismic Denoising Using Higher-Order Statistics and Improved Wavelet Block Thresholding, Bull. Seismol. Soc. Am., 106(4), 1380-1393.

Mousavi, S. M., Langston, C. A. & Horton, S. P., 2016. Automatic micro-seismic denoising and onset detection using the synchrosqueezed-con- tinuous wavelet transform, Geophysics, 81(4), 1–15, doi: 10.1190/ GEO2015-0598.1.

Nyamwandha, C. A., Powell, C. A. & Langston, C. A., 2016. A joint local and teleseismic tomography study of the Mississippi Embayment and New Madrid Seismic Zone, J. Geophys. Res. B Solid Earth Planets, 121(5), 3570-3585.

Pazos, A., Gonzalez, M. J. & Alguacil, G., 2003. Non-linear filter using the wavelet transform applied to seismological records, J. Seismol., 7, 413–429.

Powell, C. A., Withers, M. M., DeShon, H. R. & Dunn, M. M., 2010. Intrusions and anomalous Vp/Vs ratios associated with the New Madrid seismic zone, J. Geophys. Res. B Solid Earth Planets, 115(B8).

Rioul, O. & Duhamel, P., 1992. Fast algorithms for discrete and continuous wavelet transforms, IEEE transactions on information theory, 38(2), 569-586.

Sabra, K. G., Gerstoft, P., Roux, P., Kuperman, W. A. & Fehler, M. C., 2005. Extracting time-domain Green's function estimates from ambient seismic noise, Geophysical Research Letters, 32(3).

Shapiro, N. M., Campillo, M., Stehly, L. & Ritzwoller, M. H., 2005. High-resolution surface-wave tomography from ambient seismic noise, Science, 307(5715), 1615-1618.

Starck, J. L., Murtagh, F. & Fadili, J. M., 2010. Sparse Image and Signal Processing. New York: Cambridge University Press.

Tary, J. B., Herrea, R. H., Han, J. & Baan, M. V. D., 2014. Spectral estimation—What is new? What is next? Rev. Geophys., 52(4), 723–749, doi: 10.1002/2014RG000461.

Thomas, W. A., 2006, Tectonic inheritance at a continental margin, GSA today, 16(2), 4-11.

To, C. A., Moore, J. R. & Glaser, S. D., 2009. Wavelet denoising techniques with applications to experimental geophysical data, Signal Process., 89, 144–160, doi: 10.1016/j.sigpro.2008.07.023.

Torrence, C. & Compo, G. P., 1998. "A practical guide to wavelet analysis." Bulletin of the American Meteorological Society, 79(1), 61-78.

Tuttle, M. P., Schweig, E. S., Sims, J. D., Lafferty, R. H., Wolf, L. W. & Haynes, M. L., 2002. The earthquake potential of the New Madrid seismic zone, Bull. Seismol. Soc. Am., 92(6), 2080-2089.

Van Arsdale, R. & Cupples, W., 2013. Late Pliocene and Quaternary deformation of the Reelfoot rift, Geosphere, 9(6), 1819-1831.

Van Arsdale, R., Bresnahan, R., McCallister, N. & Waldron, B., 2007. Upland Complex of the central Mississippi River valley: Its origin, denudation, and possible role in reactivation of the New Madrid seismic zone, Geological Society of America Special Papers, 425, 177-192.

Wapenaar, K. & Fokkema, J., 2006. Green’s function representations for seismic interferometry, Geophysics, 71(4), SI33-SI46.

Weaver, J. B., Yansun, X., Healy, D. M. & Cromwell, L. D., 1991. Filtering noise from images with wavelet transforms, Matnetic Resonance in Medicine, 21, 288-295.

Yang, Y. & Langston, C. A., 2019. Full waveform ambient noise tomography for the northern Mississippi embayment, unpublished manuscript.

Yao, H., van Der Hilst, R. D. & De Hoop, M. V., 2006. Surface-wave array tomography in SE Tibet from ambient seismic noise and two-station analysis—I. Phase velocity maps, Geophys. J. Int., 166(2), 732-744.

FIGURES

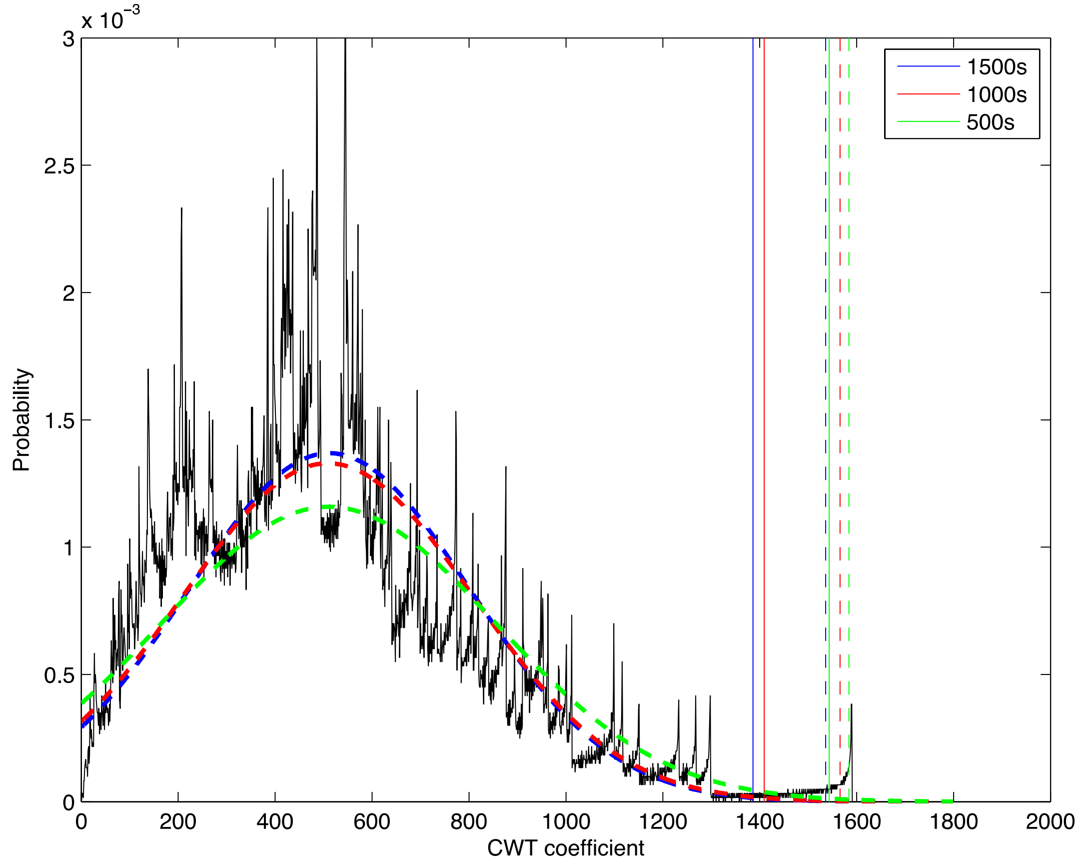

Figure 1. Empirical probability density function of the ambient noise CWT coefficients (black line) and the estimated probability density function (dashed line) with the assumption of normal distribution. The ambient noise data used for this plot are shown in the synthetic test figure. The empirical probability density function is plotted only with 1500s data and the noise level is estimated with different data length of 1500s, 1000s and 500s, respectively. The vertical solid line and dashed line show the estimated noise level based on Gaussian distribution and empirical probability distribution with 99% confidence value, respectively. Notice that the estimated noise level is more stable with ECDF method.

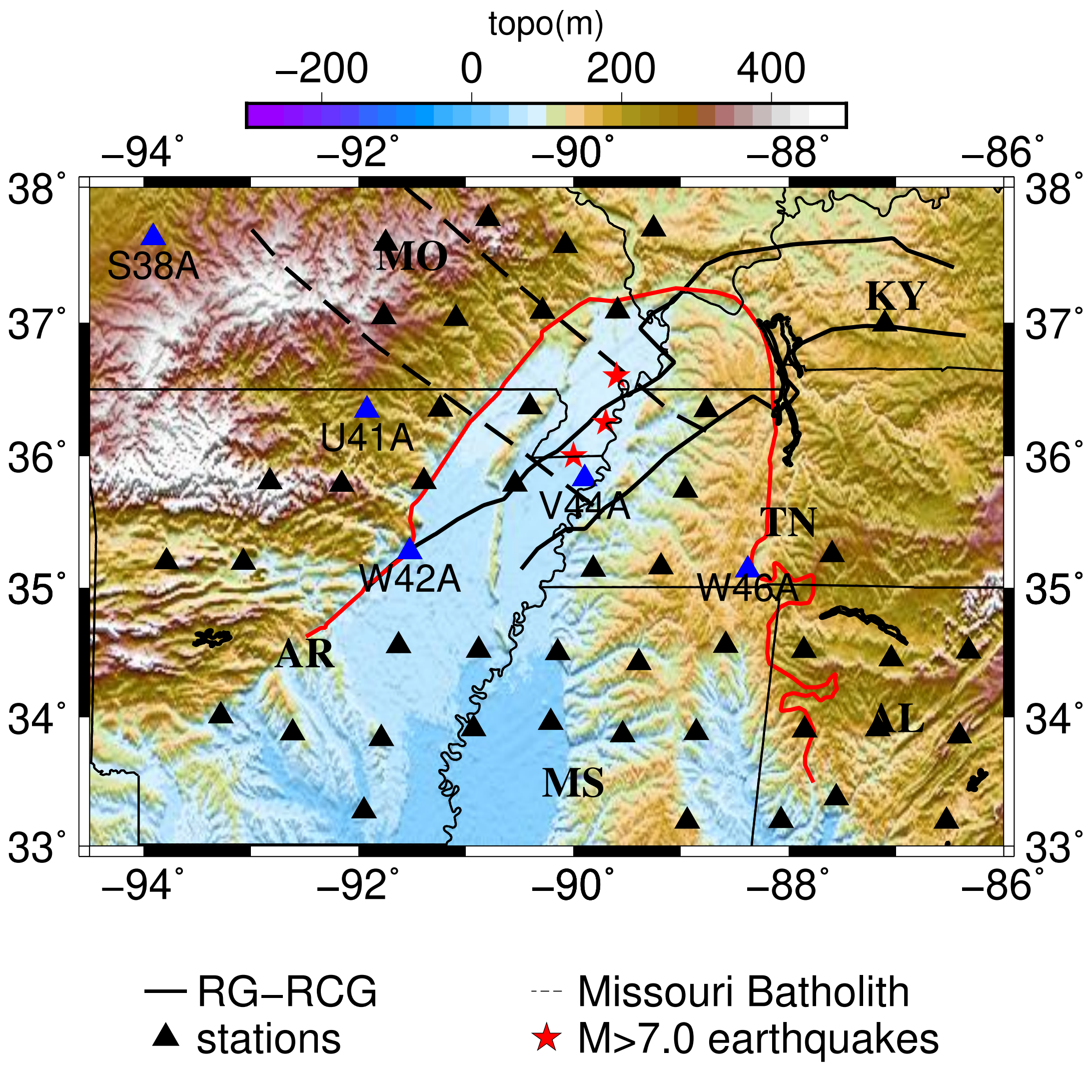

Figure 2. The distribution of the seismic stations used in this study (filled triangles). Continuously seismic recordings during July 2012 from a subset of the USArray Transportable Array stations in and around the northern Mississippi embayment are our benchmark test dataset. Major geological features include the Reelfoot Graben (RG), Rough Creek Graben (RCG) and Missouri batholith (between two dashed lines). The boundary of the Mississippi embayment is shown by the red lines. The locations of the three large earthquakes that occurred in 1811 and 1812 are shown as the red stars (Johnston & Schwieg, 1996). Several specific stations used as examples in the rest of this article are annotated.

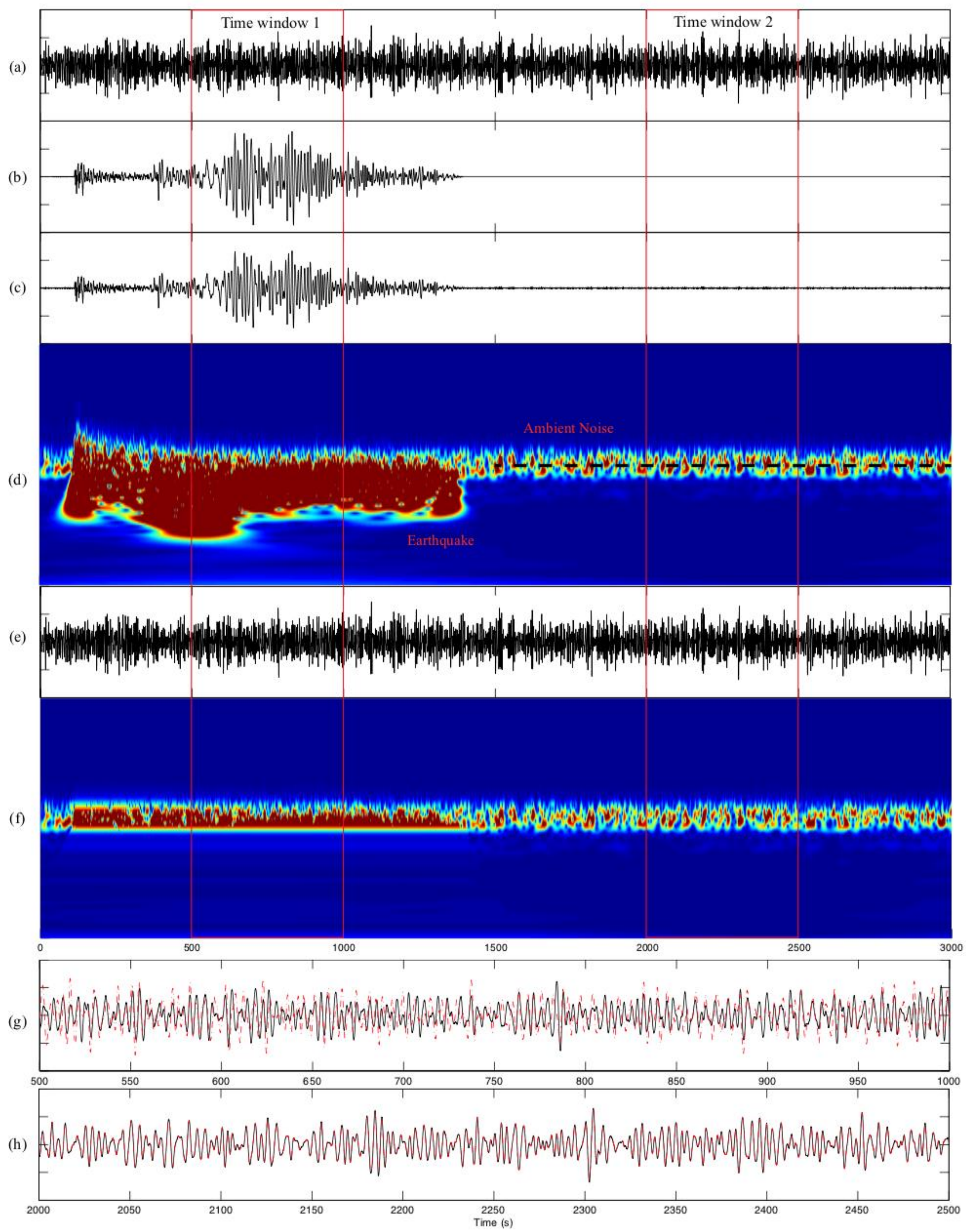

Figure 3. Designaling synthetic test based on recorded ambient noise and earthquake data. (a) 3000s ambient noise data from station U41A. (b) The July 25, 2012, teleseismic earthquake recorded by station U41A. The data are denoised with the CWT soft thresholding denoising

algorithm and a 1Hz low-pass filter is applied after denoising. Data before the first arrival and after 1400 seconds are tapered. (c) Synthetic data constructed by summing ambient noise data in (a) and seismic event data in (b). (d) The modulus of the complex CWT spectrum of synthetic data in (c). The dashed line indicates the data used in (a). (e) Synthetic data after designaling shown in the time domain. (f) Synthetic data after designaling shown in the CWT domain. (g) The comparison of seismic data before designaling (solid line) and after designaling (dashed line) with the data in the time window 1. (h) Same as (g) but for time the window 2. The vertical red lines delineate the two 500s time windows.

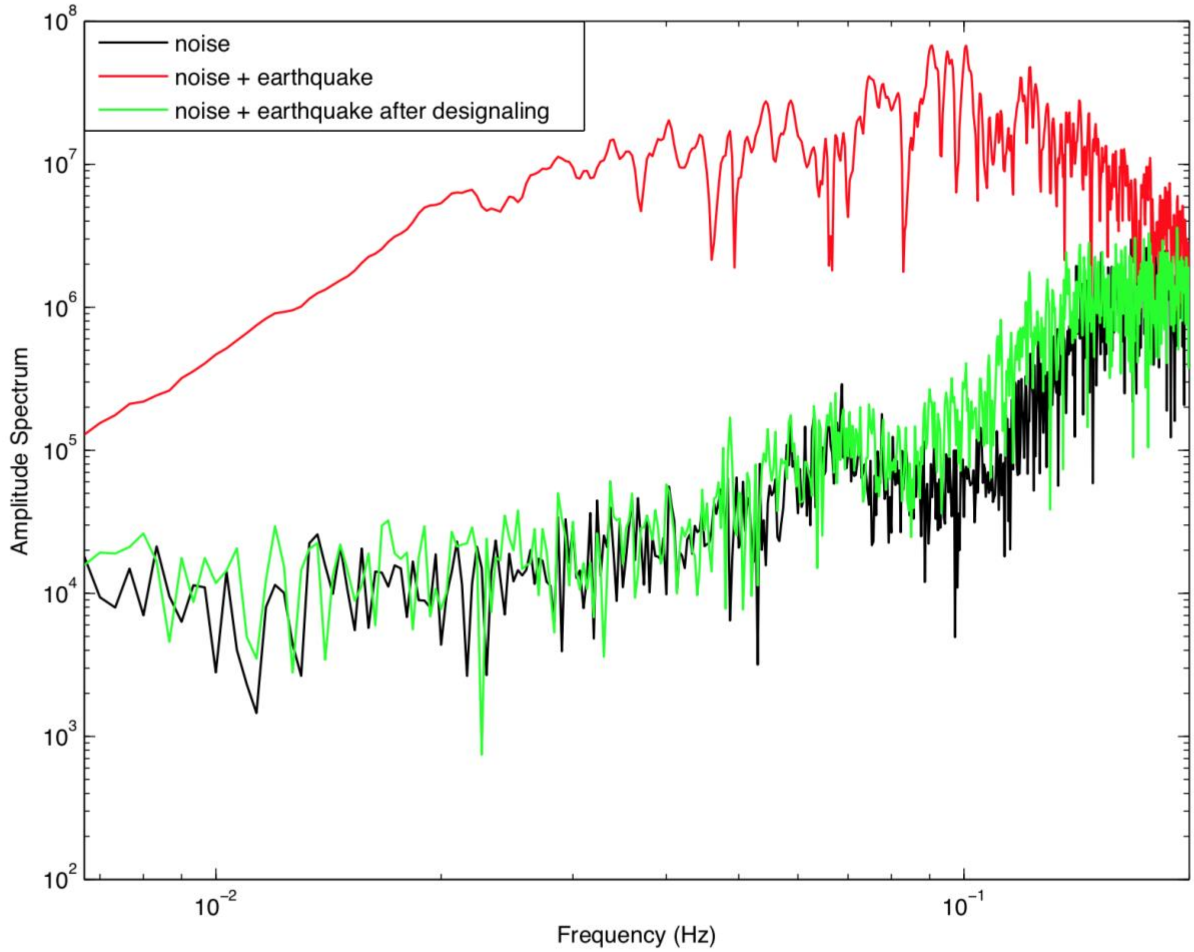

Figure 4. The comparison of the Fourier amplitude spectrum between the original noise data, the noise data added with earthquake data and the final designaled data.

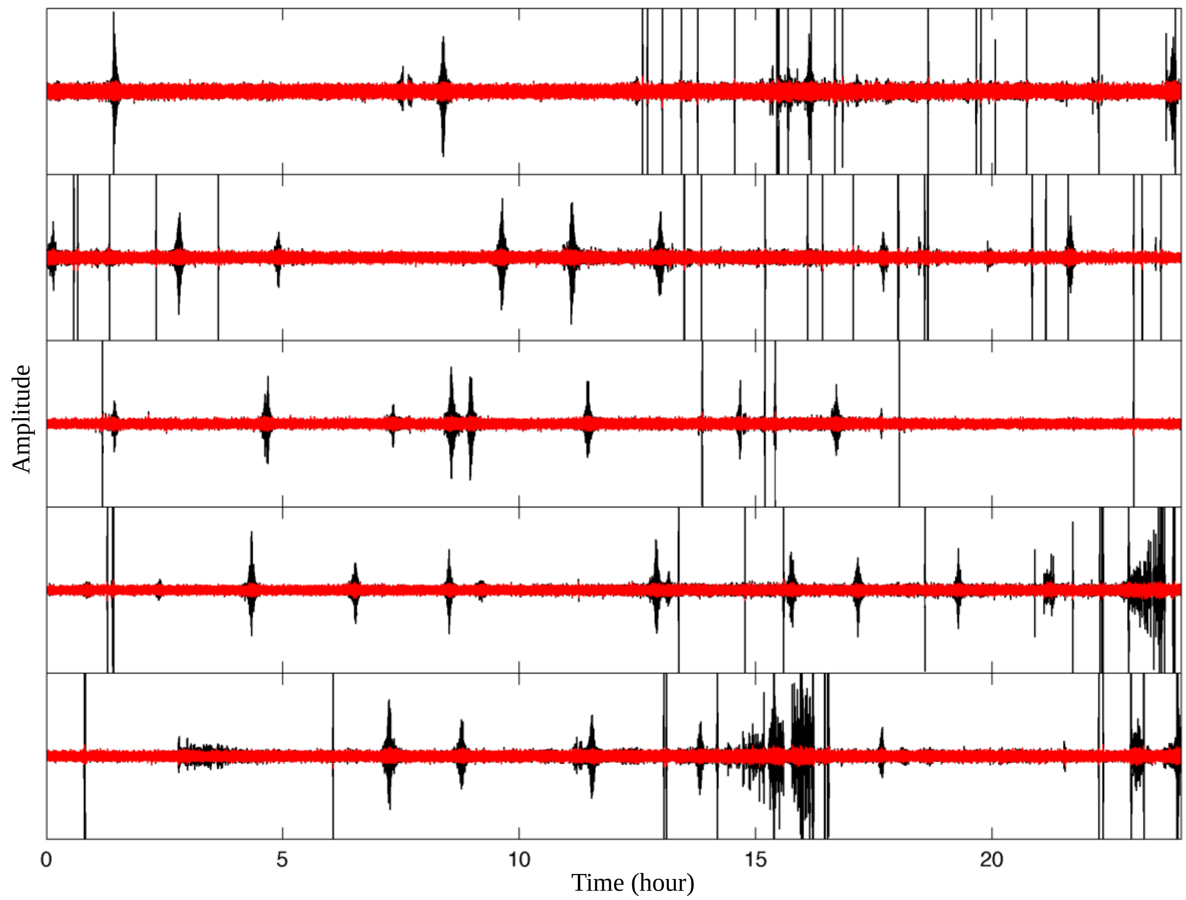

Figure 5. Vertical component seismograms of station V44A recorded during the first five-days of July 2012 (black) and the designaled result (red). Each row shows one-day of seismic data. There are many earthquakes and transient signals recorded by the station. These signals are successfully removed after designaling.

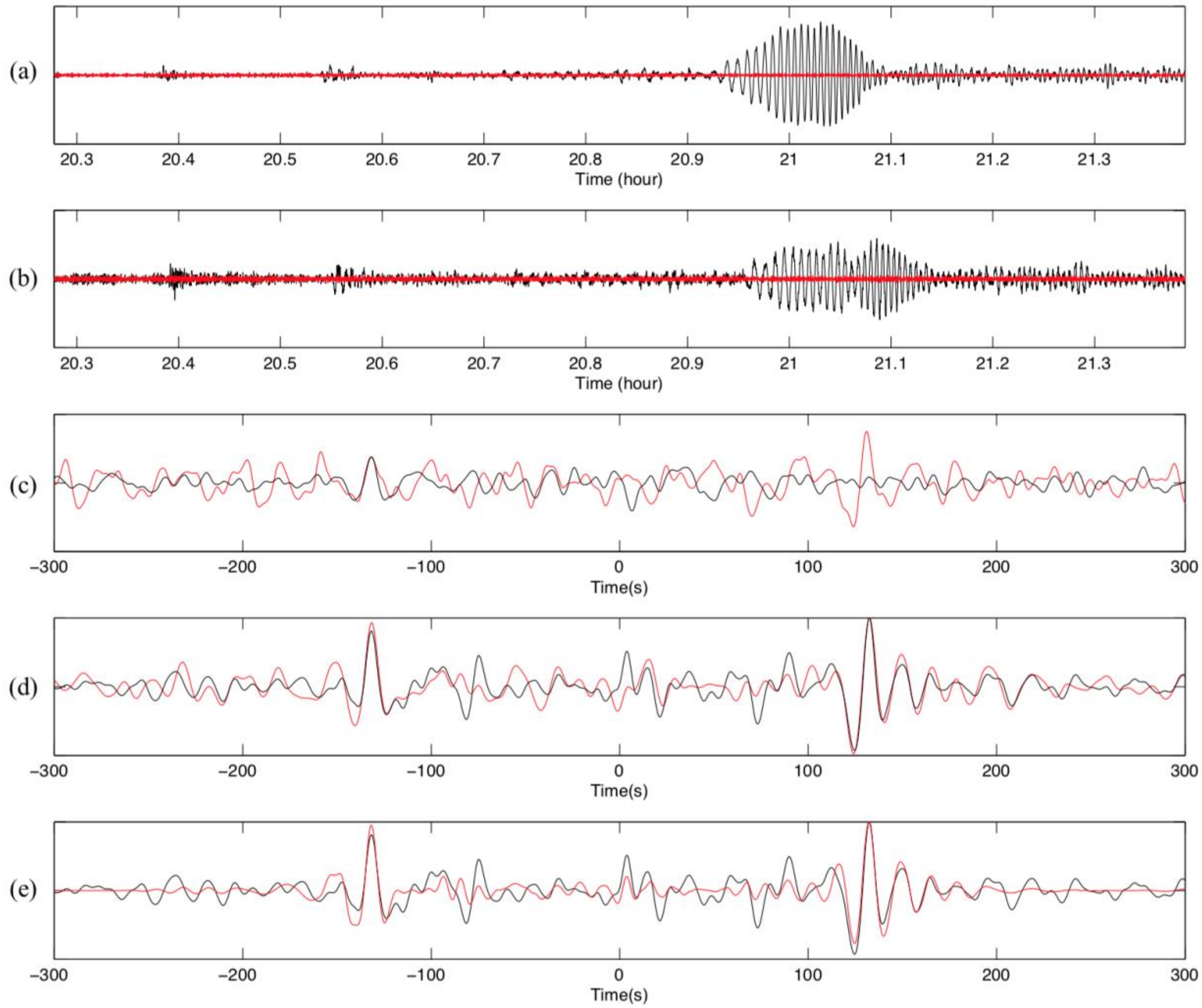

Figure 6. EGF calculation between station V44A and S38A. (a) A segment of seismic record for station S38A on July 28, 2012, with the black line indicating the original data and the red line showing the designaled results. A teleseismic event is seen within this time period and is removed after designaling. (b) Same as (a) but for station V44A. (c) One-day cross-correlation between station S38A and station V44A for date July 28, 2012, calculated using TDN (black) and the designaled data (red). (d) One-month stacked cross-correlogram obtained from TDN (black) and our processing flow before the final denoising step (red). (e) One-month stacked cross-correlogram obtained from TDN and our processing after the final denoising step (red). Absolute amplitude is plotted in (c). The amplitude is normalized in (d) and (e).

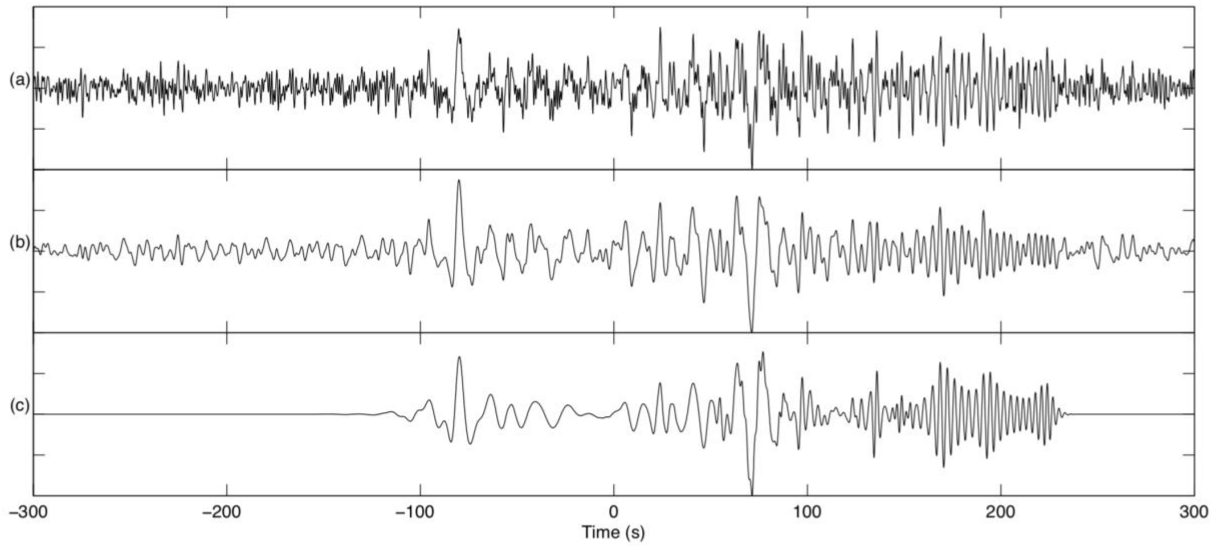

Figure 7. Application of soft threshold denoising on the final stacked cross-correlogram for stations W42A and W46A. (a) Original stacked cross-correlogram. (b) Stacked cross-correlogram with a 0.3Hz low-pass filtered applied. (c) Stacked cross-correlogram after soft thresholding denoising.

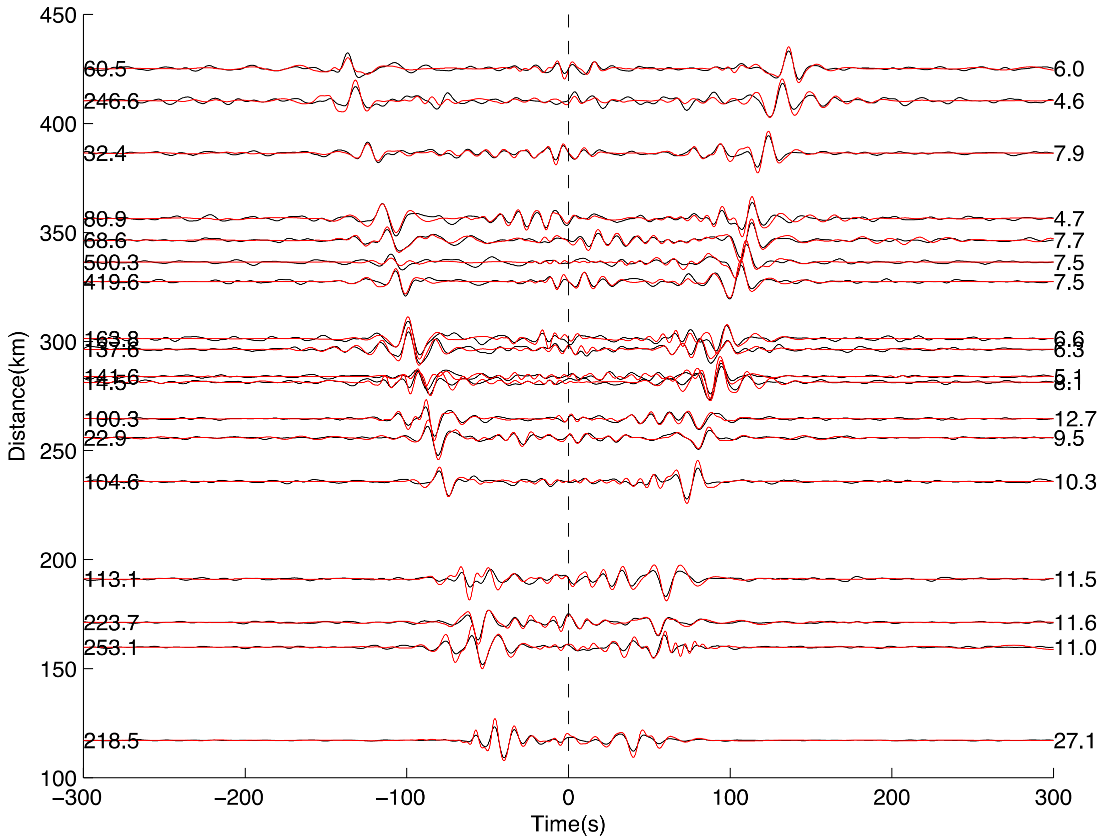

Figure 8. EGFs record section acquired from TDN (black) and our processing flow (red) for station V44A. SNR for the results from TDN is shown on the right side and for our method on the left side. The SNR is calculated using the ratio between the maximum amplitude from the time window -200s to 200s and maximum amplitude of the remaining part. A bandpass filter between 0.01s and 0.15s is applied to all data. The amplitude is the stacked absolute amplitude without normalization.

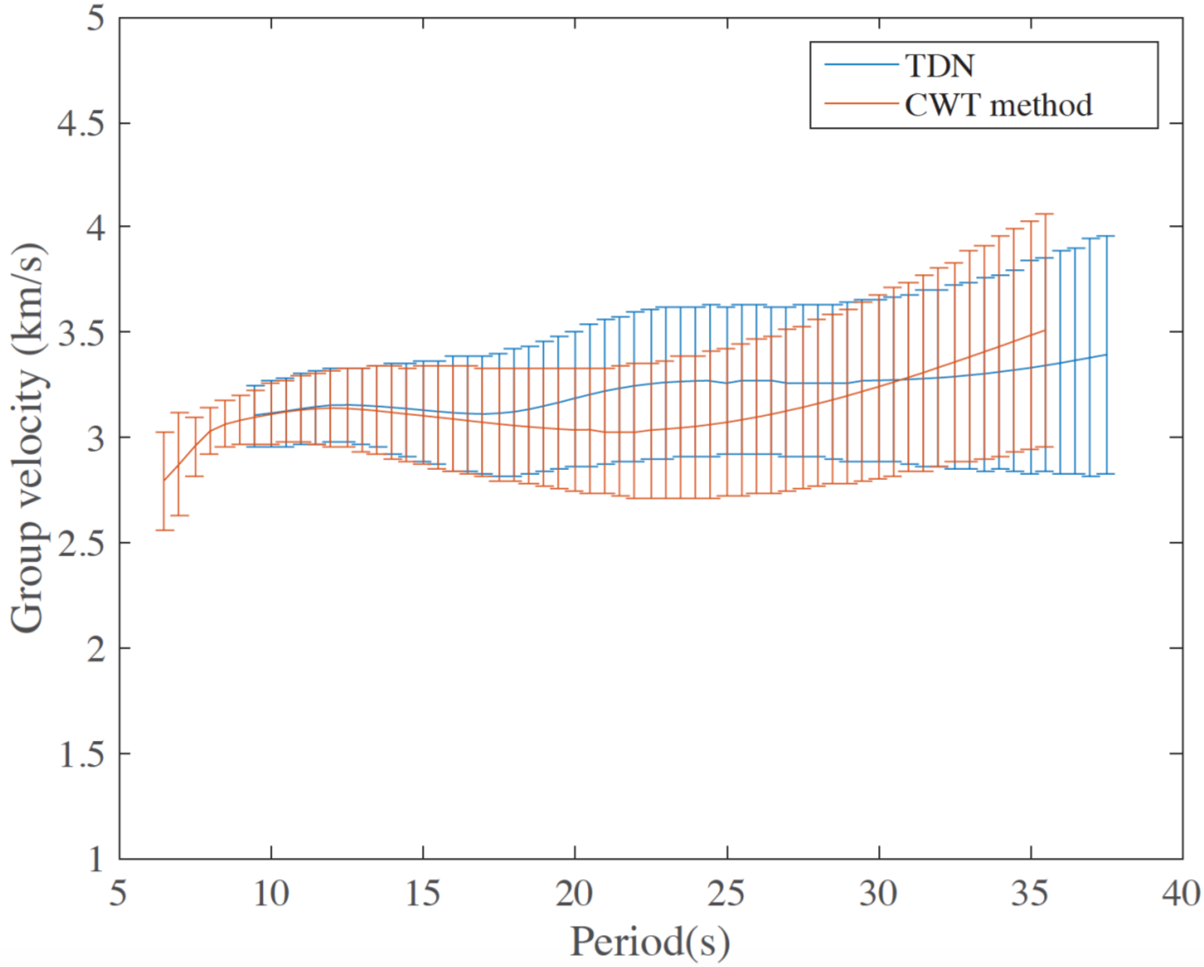

Figure 9. Comparison of group velocity dispersion curves from station V44A to station S38A from an EGF using TDN (blue) and our processing flow (red).